Electronic Supplementary Material (ESI) for ChemComm.

SUPPORTING INFORMATION

Enzyme Activity Evaluation by Differential Electrochemical Mass Spectrometry

*João C. P. de Souza[a,b], Wanderson O. Silva[a], Fabio H. B. Lima[a] and Frank N. Crespilho[a]**

a- São Carlos Institute of Chemistry, University of São Paulo, São Carlos-SP, Brazil 13560-970
b- Goiano Federal Institute, Rio Verde-GO, Brazil 75901-970

**E-mail: frankcrespilho@iqsc.usp.br*

Summary

1. Experimental Procedures

1.1 Materials

Alcohol dehydrogenase (ADH) from *Saccharomyces cerevisiae* was purchased from Sigma-Aldrich. The arrays of flexible carbon fibers (FCF) were extracted from the carbon cloth CCS 200. Potassium permanganate and sulfuric acid, used in the FCF treatment, were purchased from Synth and Sigma-Aldrich, respectively. Nafion® and absolute ethanol were purchased from Sigma-Aldrich. Phosphate salts for buffer preparation were purchased from Synth. Polytetrafluoroethylene (PTFE) membrane with 0.02 µm porous size was obtained from Gore-Tex®.

1.2 Chemical treatment of flexible carbon fibers

0.5 g of FCF was immersed in 120 mL of solution composed by 1.0 mol L^{-1} H_2SO_4 and 24.5 mol L^{-1} $KMnO_4$. This mixture was kept in an ultrasound bath for 3 hours. The FCF was removed from this system and then washed with HCl (37%) until to remove residual MnO_2, and then cleaned with ultrapure water to remove the acid residues. This treatment promotes the formation of quinone-like groups on fiber surface, which is well-known for catalyze the electrooxidation of β-nicotinamide adenine dinucleotide (NADH).[1] The pristine and treated FCF were characterized by field emission gun scanning electron microscope (FEG-SEM) and energy dispersive spectroscopy (EDS). Figure S1 presents FEG-SEM images of pristine (a) and treated FCF (b). We can observe the increase of the surface roughness that was provided by the fiber oxidation.

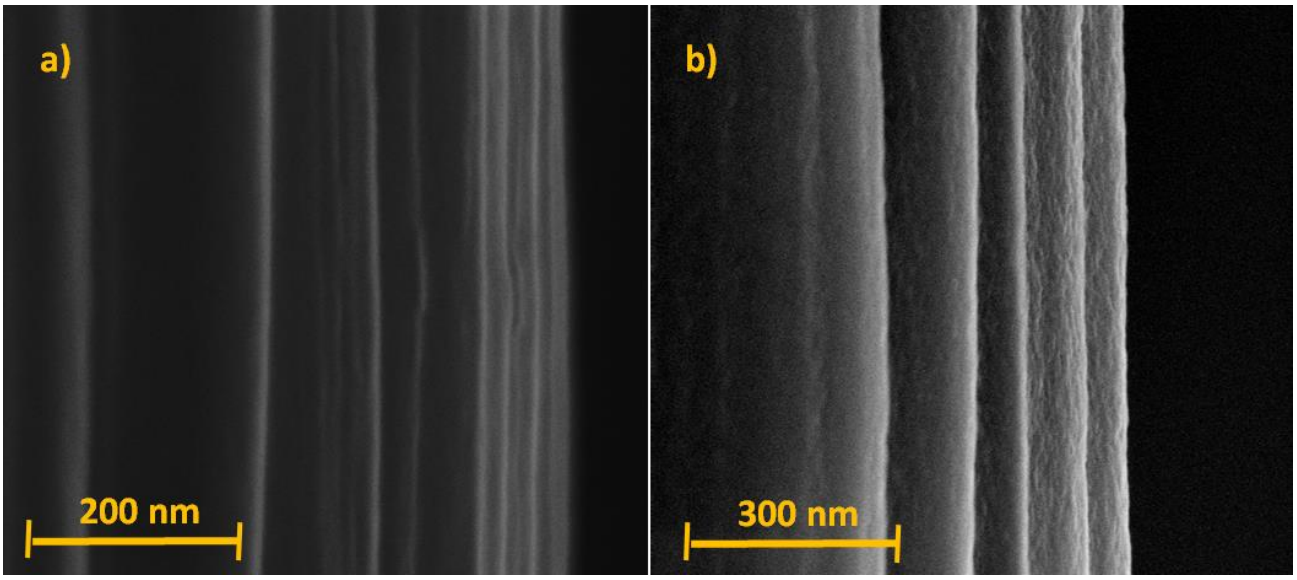

Figure S1 - **a)** Pristine flexible carbon fiber and **b)** treated flexible carbon fiber and evidence of increase of surface roughness.

The EDS elementary microanalysis revealed that the oxidizing treatment of the FCF increased the percentage of the superficial oxygen in their composition (table S1). Also, in a recent study we used x-ray photoelectronic spectroscopy (XPS)[1] to show the increase of oxygen and oxygenated carbon functional groups, which was related as quinone-like groups formation.

Table S1. Elementary composition obtained by EDS of pristine FCF and treated FCF.

FCF	Carbon (%)	Oxygen (%)
Pristine	99 %	1%
Treated	97%	3%

1.3 Bioelectrode: Enzyme immobilization

After the fiber treatment, the FCF-ADH bioelectrode was obtained by physical adsorption of the enzyme by dropping 200 µL of 16 mg mL^{-1} of ADH on FCF array (0.9 cm^2) and kept for five hours on the fridge. Posteriorly, 20 µL of Nafion® 5% solution was added atop of FCF-ADH and it was kept under vacuum in desiccator during one hour. Figure S2 shows the support of the working electrode (FCF-ADH), where there is a gold wire with a ring that promote the electrical contact with FFC-ADH bioelectrode. Under the FCF array, it is located the PTFE membrane, supported on a stainless steel frit, that is used as the permeable interface with the DEMS equipment for gaseous or volatile product detection.

1.4 Electrodes connection

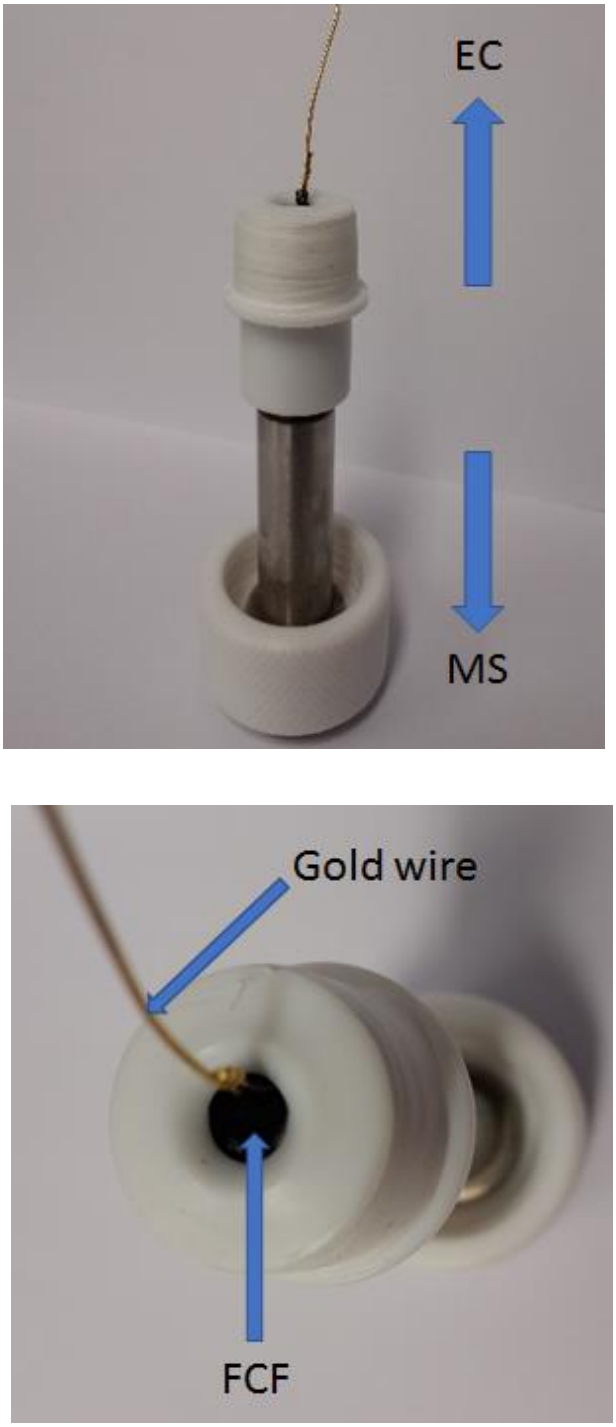

Figure S2. Steel part that connects the electrochemical cell and the mass spectrometer. The working electrode is on the top, in which the electrical contact is connected by a gold wire.

1.5Differential electrochemical mass spectroscopy (DEMS)

The DEMS technique allows the on-line detection of volatile and gaseous products from bioelectrochemical reactions. The figure S3 the photography of the home-made equipment: 1) the home-made electrochemical cell; 2) pre-vacuum chamber where the volatile compounds are in gaseous phase; 3) turbomolecular pump of the pre-vacuum chamber; 4) quadrupole analyzer; 5) turbomolecular pump of the main chamber; 6) valves; 7) electronic controller and 8) the computer. The quadrupole mass spectrometer is a Pfeiffer Vacuum QMA 200 and two differentially pumping chambers. The electrochemical potential was recorded simultaneously with the mass intensity, for selected values of m/z (mass/charge) ionic signals, which are m/z 22 and 29. A high area platinum electrode and a $Ag/AgCl/Cl^-_{sat}$ served as counter and reference electrodes, respectively. FCF-ADH was used as working electrode. The electrochemical system was controlled by the Potentiostat/Galvanostat Autolab, PGSTAT 128N.

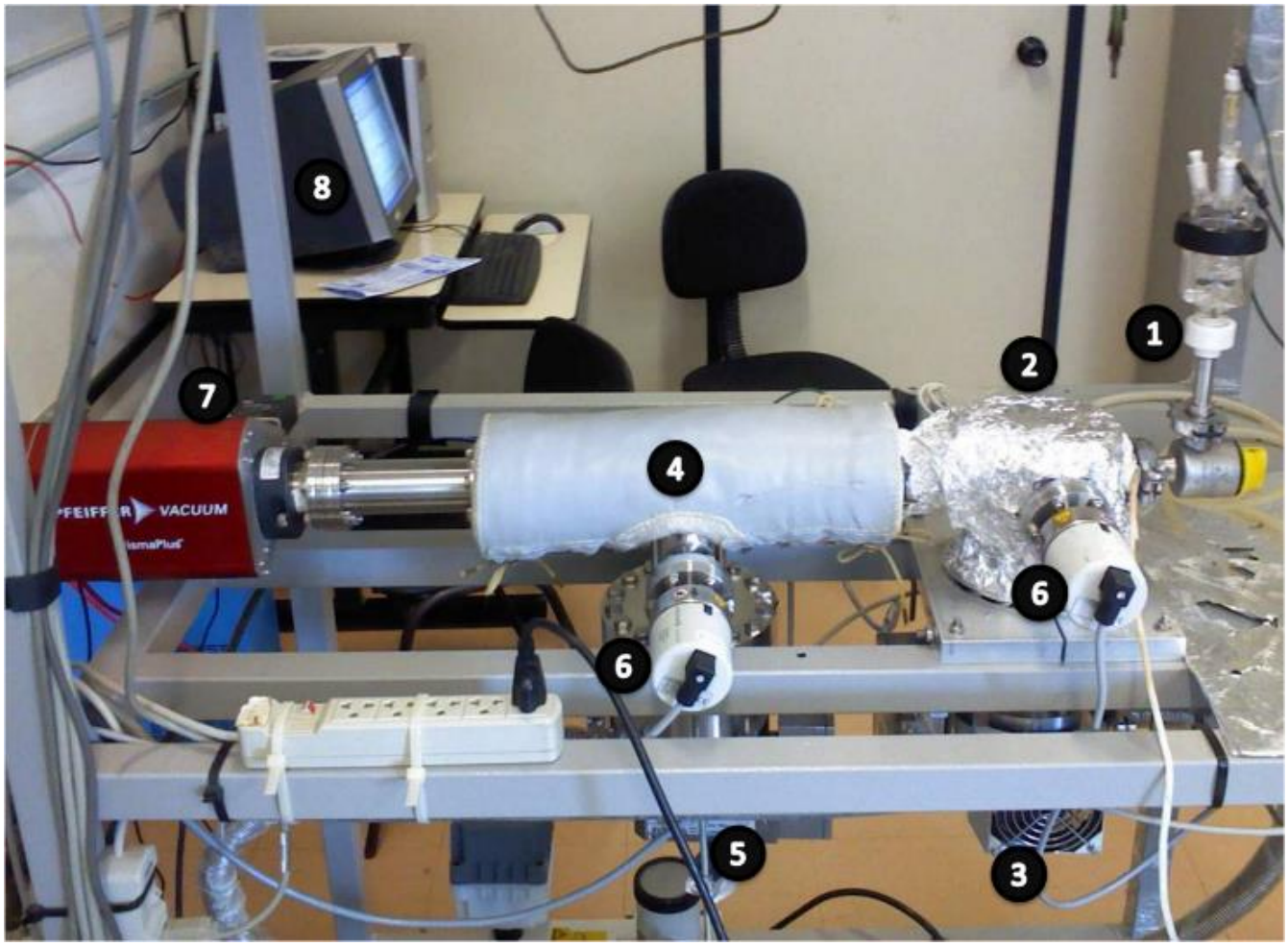

Figure S3 - DEMS equipment setup 1) electrochemical cell 2) pre-vacuum chamber, 3) turbomolecular pump of the pre-vacuum chamber 4) quadrupole analyzer, 5) turbomolecular pump of the main chamber 6) valves 7) electronic controller e 8) computer.

1.6 DEMS electrochemical cell for bioelectrocatalysis

The cell was based on a conventional electrochemical cell, but with an aperture on the bottom of the flask for fitting the working electrode with stainless steel tube that connects electrochemical cell and the mass spectrometer.

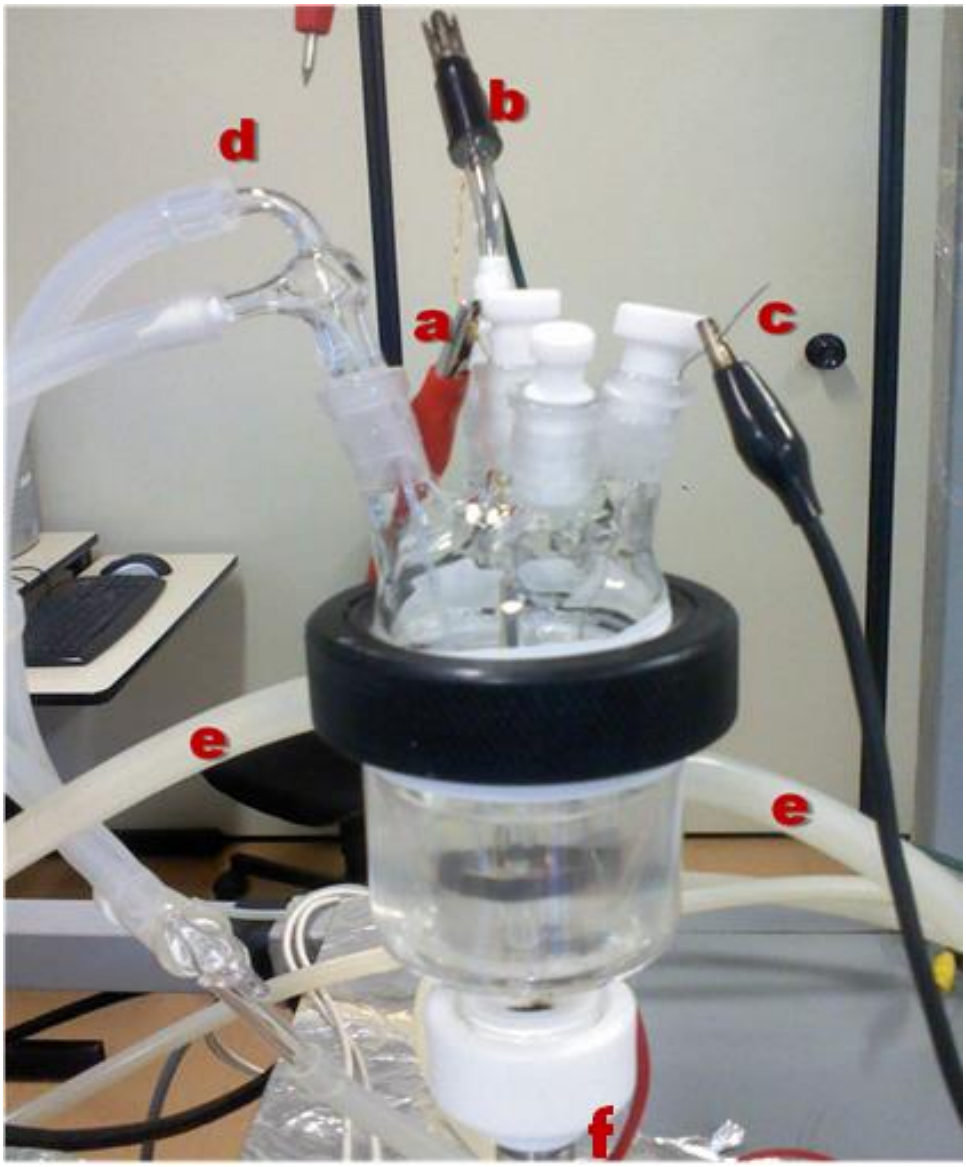

Figure S4 - DEMS electrochemical cell a) working electrode b) reference electrode c) counter electrode d) gas inlet e) temperature controller f) steel part that connects electrochemical cell and the mass spectrometer.

1. Results and Discussion

2.1 Alcohol dehydrogenase (ADH): Kinetics

ADH from *Saccharomyces cerevisiae*is is a homotetramer of subunits with 347 amino acid residues, the structure of ADH is presented in the figure S5 (PDB 5ENV and Plapp et al.).[2]

a) **b)**

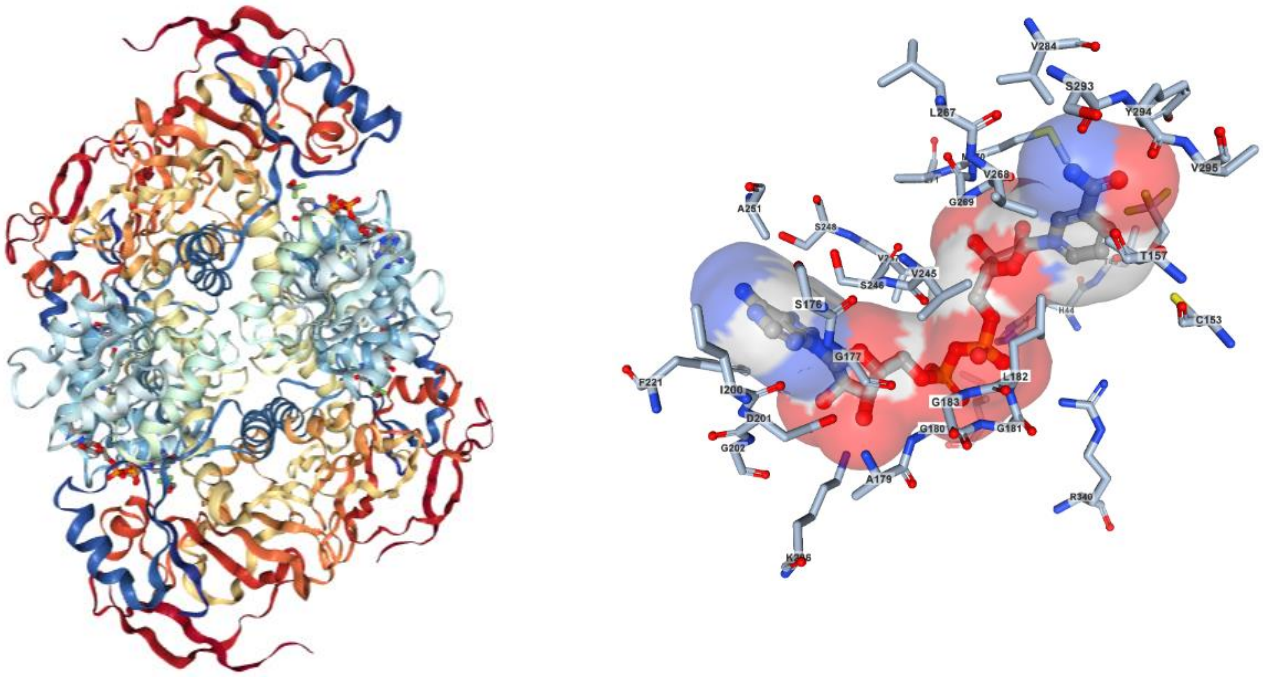

Figure S5 - **a)** Alcohol dehydrogenase structure **b)**active site with NAD^+ bound.

ADH catalyzes the oxidation of primary alcohols into aldehydes in a reversible way, and the NAD^+ is reduced to NADH. NAD^+ binds first followed by the substrate[3] in a bisubstrate enzymatic reaction. Bisubstrate can be divided in five types: ordered Bi Bi, iso-ordered Bi Bi, ping-pong Bi Bi, Theorel-Chance and random Bi Bi mechanism[4]. The ADH follow the bi-bi ordered sequential during the ethanol oxidation catalysis. Figure S6 presents the steps involved in the ADH mechanism proposed by

Dickenson and Dickinson.[5] In this model, NAD^+ probably is the first to bind in the enzyme structure ($ADH\text{-}NAD^+$),with subsequent substrate binding (ADH-ethanol), thereby forming a ternary complex ($ADH\text{-}NAD^+$-ethanol). The rate-limiting step of ethanol oxidation at neutral pH, but the dissociation of NADH from the ADH-NADH complex (k_7).

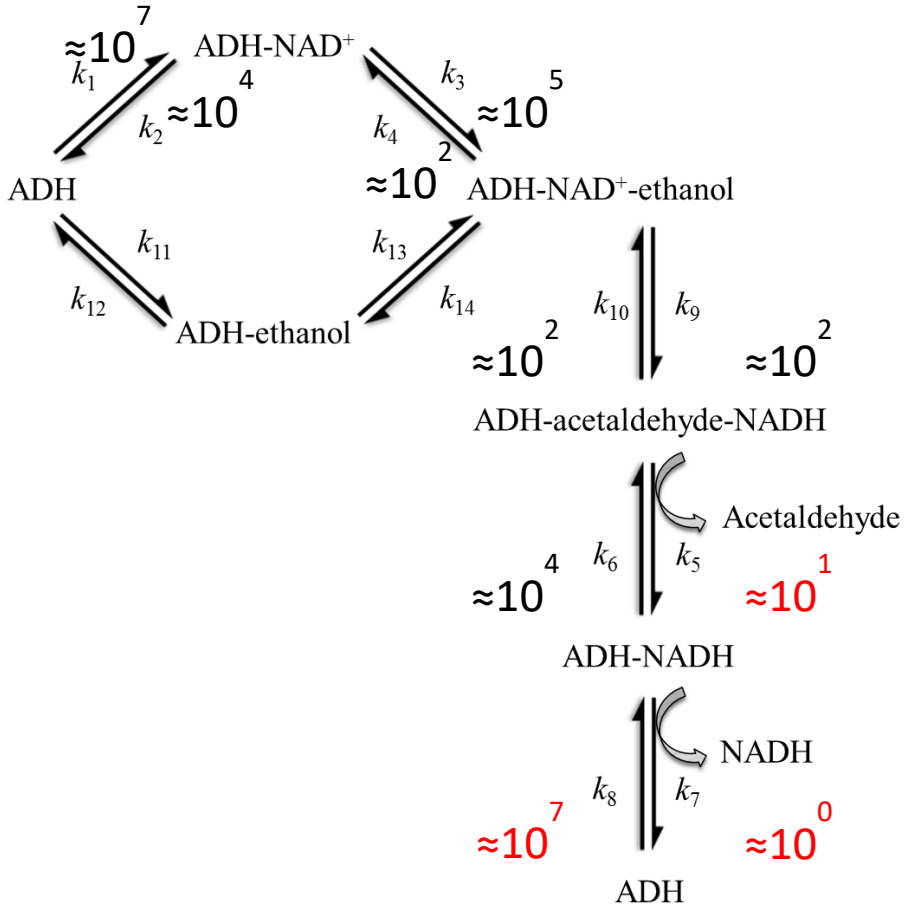

Figure S6. Mechanism for ADH enzyme. This is an illustrated rereading of the mechanism proposed pioneering by Dickenson and Dickinson[5], where the authors carried out the kinetics of ethanol oxidation by NAD^+, and acetaldehyde and butyraldehyde reduction by NADH. The constants magnitudes are expressed beside reaction step, and these values were based on reference 6 and 7. The values of rate constants were obtained by stopped-flow techniques.

The Michaelis-Menten kinetics was used for NAD^+ and ethanol reactions for ADH. We can compare kinetics of the both sites by using the double reciprocal plot, which is given from equation 1:

$$\frac{1}{V_0} = \frac{1}{V_{max}} + \frac{1}{[S]}\frac{K_m}{V_{max}} \qquad (1)$$

where V_0 is the reaction rate, V_{max} is the maximum reaction rate, [S] is substrate concentration and K_m is the Michaelis-Menten constant. For steady-state current obtained from chronoamperometry, the faradaic current is used to estimate kinetic parameters for NADH oxidation[8-10], by following equation 2:

$$\frac{1}{I_{ss}} = \frac{1}{I_{max}} + \frac{1}{[S]}\frac{K_m^{app}}{I_{max}} \qquad (2)$$

where I_{SS} is the steady-state current after the addition of substrate, I_{max} is the maximum current measured under saturated substrate conditions, [S] is the concentration of substrate in the bulk, and K_m^{app} is apparent Michaelis-Menten constant. In a similar way, when it is used differential electrochemical mass spectroscopy, the ionic current can be used in equation 2, which corresponds to acetaldehyde formation. Thus, we can compare the slope of double reciprocal plots figure 2e and 2f in the manuscript, in order to obtain the K_m^{app}/I_{max}.

3. References

1 A. R. Pereira, J. C. P. de Souza, A. D. Gonçalves, K. C. Pagnoncelli, F. N. Crespilho, J. Braz. Chem. Soc.,2017, in press. DOI: 10.21577/0103-5053.20170012

2 B. V. Plapp, H. A. Charlier, S. Ramaswamy, Archives of biochemistry and biophysics, 2016, **591**, 35-42.

3 H. Theorell, B. Chance, Acta Chem. Scand., 1951, **5**, 1127-1144.

4 J. Yon-Kahn, G. Hervé, Molecular and cellular enzymology, vol. 1 Springer Science & Business Media, 2009.

5 C. J. Dickenson, F. M. Dickinson, Biochem. J.,1975, **147**, 303.

6 B. V. Plapp, Archives of biochemistry and biophysics, 2010, **493**, 3-12.

7 V.C. Sekhar, B.V. Plapp, Biochemistry, 1990, **29**, 4289–4295.

8 A. E. G. Cass, *Biosensors: A Practical Approach*; IRL Press: Oxford, 1990.

9 Nasri, Z.; Shams, E.; Ahmadi, M.; Electroanalysis*,* 2013, **25**, 1917.

10 J. Li, S. N. Tan, H. Ge, Anal. Chim. Acta, 1996, **335**, 137.